Cytochrome P450-Mediated Cyclization in Eunicellane-Derived Diterpenoid Biosynthesis

Zengyuan Wang,[1,5] Qian Yang,[1,5] Jingyi He,[1] Haixin Li,[1] Xingming Pan,[1] Zining Li,[3] Hui-Min Xu,[4] Jeffrey D. Rudolf,[3] Dean J. Tantillo,[2]* and Liao-Bin Dong[1]**

[1]State Key Laboratory of Natural Medicines, School of Traditional Chinese Pharmacy, China Pharmaceutical University, Nanjing 211198, Jiangsu, China

[2]Department of Chemistry, University of California, Davis, California 95616, United States

[3]Department of Chemistry, University of Florida, Gainesville, Florida 32611-7011, United States

[4]The Public Laboratory Platform, China Pharmaceutical University, Nanjing 211198, China

[5]These authors contributed to this work equally

Key Words: terpene cyclization, cytochrome P450, eunicellane-derived diterpenoids, terpenoid biosynthesis

Corresponding to: yangqian117@cpu.edu.cn (Q.Y.), djtantillo@ucdavis.edu (D.J.T.), or ldong@cpu.edu.cn (L.-B.D.)

Abstract

Terpene cyclization, one of the most complex chemical reactions in nature, is generally catalyzed by two classes of terpene cyclases (TCs). Cytochrome P450s that act as unexpected TC-like enzymes are known but are very rare. Here, we genome-mined a cryptic bacterial terpenoid gene cluster, named *ari*, from the thermophilic actinomycete strain *Amycolatopsis arida*. By employing a heterologous production system, we isolated and characterized three highly oxidized eunicellane-derived diterpenoids, aridacins A–C (**1–3**), that possess a rare 6/7/5-fused tricyclic scaffold. *In vivo* and *in vitro* experiments systematically established a non-canonical two-step biosynthetic pathway for diterpene skeleton formation. First, a class I TC (AriE) cyclizes geranylgeranyl diphosphate (GGPP) into a 6/10-fused bicyclic *cis*-eunicellane skeleton. Next, a cytochrome P450 (AriF) catalyzes cyclization of the eunicellane skeleton into the 6/7/5-fused tricyclic scaffold via C2-C6 bond formation. Quantum chemical computations support a hydrogen abstraction and subsequent oxidation mechanism for AriF catalyzed carbocation cyclization. The biosynthetic logic of skeleton construction in the aridacin diterpenoids is unprecedented, expanding the catalytic capacity and diversity of P450s and setting the stage to investigate the inherent principles of carbocation generation by P450s in the biosynthesis of terpenoids.

Introduction

The eunicellanes, a unique subfamily of diterpenoids that contain more than 360 examples, are mainly found in Octocorallia soft corals with only a few known members isolated from plants and bacteria.[1–8] Structurally, all eunicellanes share a 6/10-bicyclic skeleton with most representatives, particularly those from corals, exhibiting diverse oxidation patterns. These structures imbue eunicellanes with promising bioactivities[1,2] with examples including the anti-inflammatory klysimplexin R,[9] the antimetastatic polyanthellin A,[10] and the potent tubulin inhibitor eleutherobin.[11] Therefore, they are fascinating targets for both chemists and biologists (**Figure 1A**). The biosynthetic logic of eunicellanes has remained poorly understood; the diterpene cyclases responsible for construction of the *cis* and *trans* 6/10-bicyclic skeletons were only recently disclosed from bacteria and corals.[3,4,8,12,13]

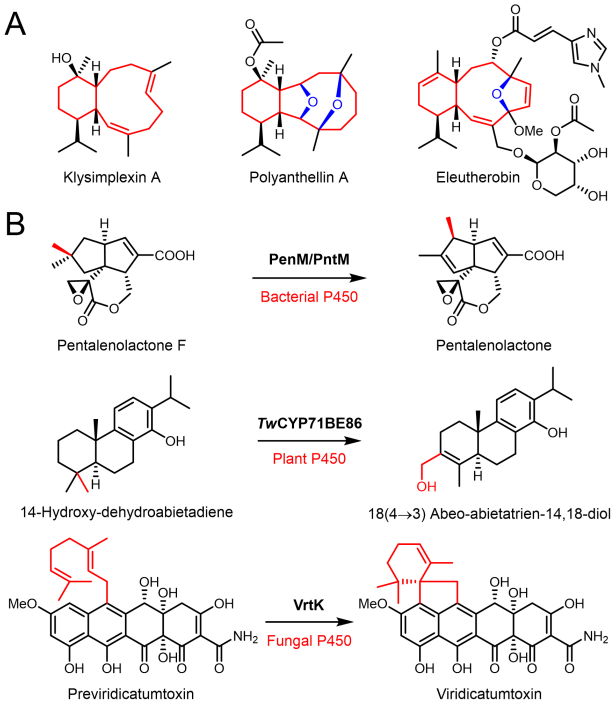

Figure 1. (A) Representative bioactive eunicellane diterpenoids; (B) P450s serve as unexpected TCs in terpenoid biosynthesis.

Terpene cyclizations are one of the most complex chemical reactions in nature. These intriguing reactions are catalyzed by a superfamily of enzymes named terpene cyclases (TCs), which utilize

nature's library of acyclic C_{5n} diphosphate precursors to generate complex mono- or polycyclic terpene skeletons via carbocation intermediates. TCs are grouped into two canonical classes according to their biochemical strategies to generate the initial carbocation: class I TCs generate carbocations by abstracting the diphosphate group and class II TCs protonate an alkene or epoxide of the prenyl diphosphate; the products of class II TCs often serve as substrates for class I TCs providing a two-step sequential route to structural diversity in terpenoid biosynthesis (**Figure S1**).[14]

Cytochrome P450 enzymes (P450s) are heme-containing monooxygenases that serve as ubiquitous tailoring enzymes that are capable of catalyzing diverse oxidation reactions including carbon-carbon bond formation in natural products biosynthesis.[15,16] P450s utilize a single-electron process to produce radical intermediates via Compound I (a high-valent oxoiron cationic radical) which readily abstracts a hydrogen from the substrate to yield reactive radical species. Typically, the radical species rapidly rebounds with the hydroxyl radical species, which is derived from molecular oxygen, to generate the hydroxylation product.[15,16] Alternatively, though rarely observed, when the rate of oxygen rebound is reduced sufficiently, an electron from the substrate can be transferred to the radical center resulting in a reactive carbocation, which can stimulate a series of cyclization or rearrangement reactions as seen in TC chemistry.[14,17] P450s that serve as TC-like enzymes are known but rare in the biosynthesis of terpenoids. The three known examples are (i) PenM/PntM catalyzing the final step of oxidative rearrangement via a neopentyl cation intermediate in the biosynthesis of the bacterial sesquiterpenoid pentalenolactone;[18,19] (ii) *Tw*CYP71BE86, a plant P450, mediating a methyl shift of the abietane-type diterpene scaffold in triptonide biosynthesis;[20] and (iii) VrtK, which resembles class II TCs and initiates cyclization in the biosynthesis of the fungal meroterpenoid viridicatumtoxin (**Figure 1B**).[21]

Here we first genome-mined for novel eunicellane diterpenoids by targeting the bacterial biosynthetic gene cluster *ari* from the thermophilic actinomycete *Amycolatopis arida*. We then

activated this cryptic biosynthetic gene cluster (BGC) by heterologous expression in model *Streptomyces* hosts and isolated three highly oxidized and eunicellane-derived 6/7/5-tricyclic diterpenoids, aridacins A−C (**1**−**3**). Their structures were unambiguously established by extensive spectroscopic analyses, including phenylglycine methyl ester (PGME) transformation and single crystal X-ray diffraction. Using a combination of heterologous production, *in vivo* inactivation, *in vitro* biochemical experiments, and quantum chemical calculations, we established that a P450, AriF, mediates the formation of the 6/7/5-tricyclic skeleton from the 6/10-bicyclic eunicellane substrate benditerpe-2,6,15-triene (**4**) via a class II-like TC mechanism.

Results and Discussion

Genome Mining Reveals a Novel Eunicellane Biosynthetic Gene Cluster. Terpenoids are the largest family of natural products with over 95,000 known compounds (http://dnp.chemnetbase.com),[22] the vast majority of which have been isolated from plants and fungi; less than 1.5% are from bacteria.[23] However, the genomes of bacteria showcase extensive terpenoid biosynthetic potential that has yet to be revealed.[23] As genes from bacterial secondary metabolism tend to be clustered together, we envisioned that targeting the gene clusters with multiple P450s neighboring TCs might be a practical approach for the discovery of highly oxidized terpenoids.[24] We targeted a putative 16-kb *ari* BGC from a thermophilic actinomycete *Amycolatopsis arida* CGMCC 4.5579 (formerly known as *Yuhushiella deserti*, **Figures 2A** and **S2**).[25,26] The *ari* BGC encodes a class I TC, a UbiA family prenyltransferase, four P450s, a ferredoxin, a geranylgeranyl diphosphate (GGPP) synthase, two genes, 4-hydroxy-3-methylbut-2-enyl diphosphate reductase (IspH) and 1-deoxy-D-xylulose 5-phosphate synthase (DXS), found in the non-mevalonate pathway, and three unknown genes (**Figures 2A** and **Table S1**). The sole TC in the *ari* BGC (named AriE) shares 71.6% protein sequence identity with Bnd4 from the benditerpenoic acid biosynthetic pathway,[8,12] suggesting that this BGC might encode eunicellane-derived diterpenoids.

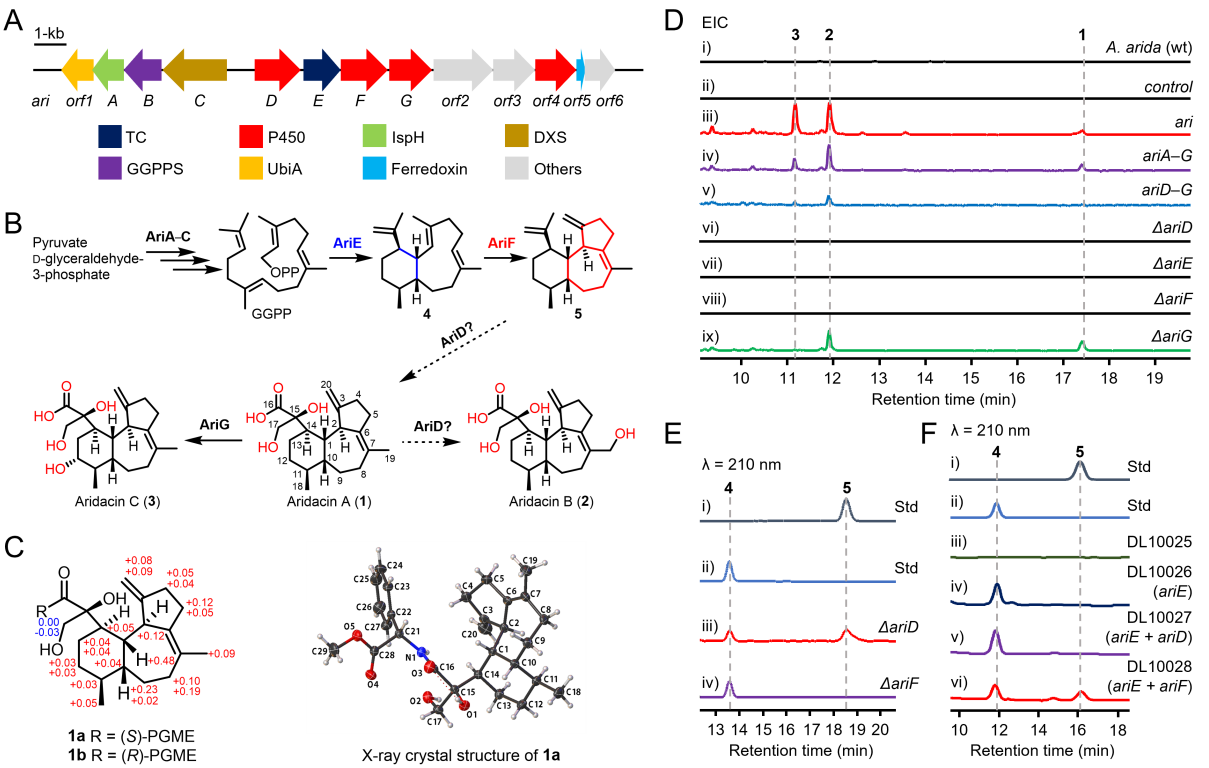

Figure 2. Biosynthesis of aridacins. (A) The *ari* biosynthetic gene cluster. (B) The proposed biosynthetic pathway of aridacins. Dashed arrows depict biosynthetic steps that were unable to be established by *in vivo* or *in vitro* experiments. (C) $\Delta\delta$ values ($\delta_{(S)} - \delta_{(R)}$) of the phenylglycine methyl ester (PGME) amides of **1a** and **1b**, and the X-ray crystal structure of **1a**. (D) EIC (333–349 *m/z*; negative mode) analysis of metabolites from engineered *Streptomyces* strains. *S. lividans* TK64 with empty pSET152 was used as a control. (E) HPLC analysis of the metabolites of Δ*ariD* and Δ*ariF* constructs in *S. lividans*. (F) HPLC analysis of the metabolites of engineered *E. coli* strains. DL10025 is a GGPP-overproducing *E. coli* strain and is used as a control. DL10026–DL10028 are DL10025 harboring *ariE*, *ariE* + *ariD*, and *ariE* + *ariF*, respectively.

Heterologous Expression of the *ari* BGC Produces Three Highly Oxidized Eunicellane-Derived Diterpenoids. Initial attempts to isolate *ari* BGC-related terpenoids from *A. arida* were unsuccessful, presumably due to the BGC being transcriptionally silent under laboratory culture conditions. To activate the *ari* BGC, we cloned and heterologously expressed it in three model *Streptomyces* hosts. *Streptomyces lividans* DL10011 (**Tables S2–S4**), which harbors the entire *ari* BGC (*orf1–orf6*), showed three new peaks (**1–3**) by HPLC-MS with *m/z* $[M-H]^-$ at 333, 349, and 349, respectively, when cultured in several terpenoid production media (**Figures 2D** and **S3–S6**).[27,28] PTMM medium provided higher titers of **2** and **3** while XTM medium was more

conducive to produce **1**.[28] Therefore, DL10011 was individually fermented on a 15-L scale in both PTMM and XTM media to isolate aridacins A–C (**1–3**, **Figure 2B**).

Aridacin A (**1**) had the molecular formula $C_{20}H_{30}O_4$ as deduced by the (–)-HRESIMS ion at *m/z* 333.2063 (calcd 333.2071), indicating six degrees of unsaturation (**Figure S7**). The ^{1}H NMR (**Figure S8** and **Table S5**) exhibited characteristic signals for two olefinic protons at δ_H (4.90 and 4.81) and two methyl groups at δ_H (1.61 and 0.90). Its ^{13}C NMR and DEPT spectra showed 20 carbon resonances including two methyls, eight methylenes, five methines, and five quaternary carbons (**Figures S9** and **S10**). The planar structure of **1**, a 6/7/5-fused tricyclic diene, was elucidated by the spin systems in the ^{1}H-^{1}H COSY spectrum of H_2-4/H_2-5 and H_2-8/H_2-9/H_1-10/H_1-11/H_2-12/H_2-13/H_1-14/H_1-1/H_1-2, and the key HMBC correlations of H-1 with C-15, H_2-17 with C-15 and C-16, and H_2-20 with C-2, C-3, and C-4 (**Figures S11–S13**). The key ROESY correlations of H-17a/H-1, H-17a/H-10, along with H-2/H-11 suggested that H-10 and H-11 were *β*- and *α*-orientated, respectively (**Figure S14**). Analyses of the NMR data of **2** and **3** concluded they were analogs of **1** (**Figures S15–S28**, and **Tables S6** and **S7**). In comparison with **1**, aridacins B (**2**) and C (**3**) have additional hydroxyl groups at C-19 and C-12, respectively (**Figure 2B**). To determine the stereochemical configuration of C-15 of the glyceric acid moiety in **1**, two derivatives, **1a** and **1b**, were synthesized using (*R*)- and (*S*)-PGME (**Figures S29–S35** and **Table S8**);[29] C-15 was determined as *S* configuration based on the $\Delta\delta$-values ($\delta_{(S)} - \delta_{(R)}$) shown in **Figure 2C**. The absolute configuration of **1a** was unambiguously determined by X-ray crystal structure (CCDC 2216506, **Figure 2C**).[30]

The aridacins A–C (**1–3**) are the first bona fide bacterial diterpenoids possessing a 6/7/5-fused tricyclic scaffold, despite the scaffold being previously seen in TC studies (**Figure S36**). Odyverdiene B was produced by heterologously expressing *nd90_0354* from *Streptomyces* sp. ND90 in a *Streptomyces* host;[31,32] isocatenula-2, 14-diene was produced by incubating GGPP with CaCS from *Catenulispora acidiphila*.[33] The highly oxidized glyceric acid moiety, which may

originate from a six-electron oxidation of the C-17 methyl group and sequential epoxidation and hydrolysis of the C-15 alkene, is also uncommon in terpenoids.[34] The aridacins A–C were screened for cytotoxicity in five cancer cells and antibacterial activity in a panel of Gram-positive and Gram-negative bacteria. However, **1–3** showed no significant biological activities (**Tables S9** and **S10**). The continued screening of other biological models is currently underway.

***In vivo* Inactivation Partially Elucidates the Biosynthetic Pathway.** To probe the biosynthetic pathway of **1–3**, we first identified the boundary of *ari* BGC (**Figures S37–S38**). We heterologously expressed *ariA–G* in *S. lividans* TK64 to yield *S. lividans* DL10016, which, based on the HPLC-MS analysis, produced equal amounts of **1–3** with that of *S. lividans* DL10011 (**Figure 2D**, panels iii and iv). This result supported that (i) *ariA–G* can be assigned putative roles in the biosynthesis of **1–3**; (ii) the UbiA-like gene (*orf1*), of which several members of this family are known as TCs, is not involved in cyclization or any other step, and (iii) three P450s genes, *ariD*, *ariF*, and *ariG*, are sufficient to decorate the diterpene skeleton. When *ariA–C* were removed (i.e., *ariD–G*), the engineered *S. lividans* DL10017 strain produced significantly less (<10%) of **2–3** than DL10011, suggestive of their important roles in precursor flux but not essential roles in the biosynthesis of the aridacins (**Figure 2D**, panel v). To further determine the function of AriD–G, we constructed a series of heterologous expression strains, each lacking one of the *ariA–G* genes in *S. lividans* DL10016 (Δ*ariD,* Δ*ariE,* Δ*ariF,* and Δ*ariG*; **Figures 2D**, panels vi–ix, and S39). In the *ariE* knockout strain (*S. lividans* DL10019), **1–3** was expectedly abolished. The Δ*ariG* mutant (*S. lividans* DL10021) only accumulated **1** and **2**, indicating AriG is responsible for installing the C-12 hydroxyl group of **3**. Both Δ*ariD* (*S. lividans* DL10018) and Δ*ariF* mutants (*S. lividans* DL10020) completely abolished the production of **1**–**3**, but intriguingly produced the highly hydrophobic products **4** and **5**, respectively (**Figures 2E** and **S40**). Due to low titers of **4** and **5** from these heterologous hosts, however, we were unable to accumulate enough material for structural elucidation.

AriE Constructs the 6/10-Fused Bicyclic *cis*-Eunicellane Skeleton. We first cloned *ariE* into our GGPP-overproduction *E. coli* system[35,36] to yield *E. coli* DL10026, and produced 20 mg of **4**. ^{1}H and ^{13}C NMR analyses confirmed its structure as the *cis*-eunicellane benditerpe-2,6,15-triene (**Figures 2F** and **S41–S43**).[8] We also cloned and heterologously produced *ariE* in *E. coli* (**Figure S44**). AriE, incubated with GGPP and Mg^{2+}, resulted in the production of **4** as well as the known 14-membered (*R*)-(–)-cembrene A (**6**, **Figures 3B** and **S45–S48**).[37,38] Compound **4** was easily transformed into a new *cis*, *trans*-6/6/6-fused tricyclic product gersemiene C (**7**) under mild acidic conditions (**Figures 3A** and **S49–S56**, and **Table S11**);[39] a similar transformation was seen for the *trans*-eunicellane albireticulene resulting in two *trans*, *trans*-6/6/6 isomers.[13] This non-enzymatic cyclization occurs via protonation at C6 of **4** followed by 2,7-annulation and deprotonation at C-20 to access **7** (**Figure S49**). Taken together, AriE merely produces the 6/10-fused bicyclic eunicellane diterpene skeleton but not the 6/7/5-fused tricyclic scaffold seen in **1**–**3**.

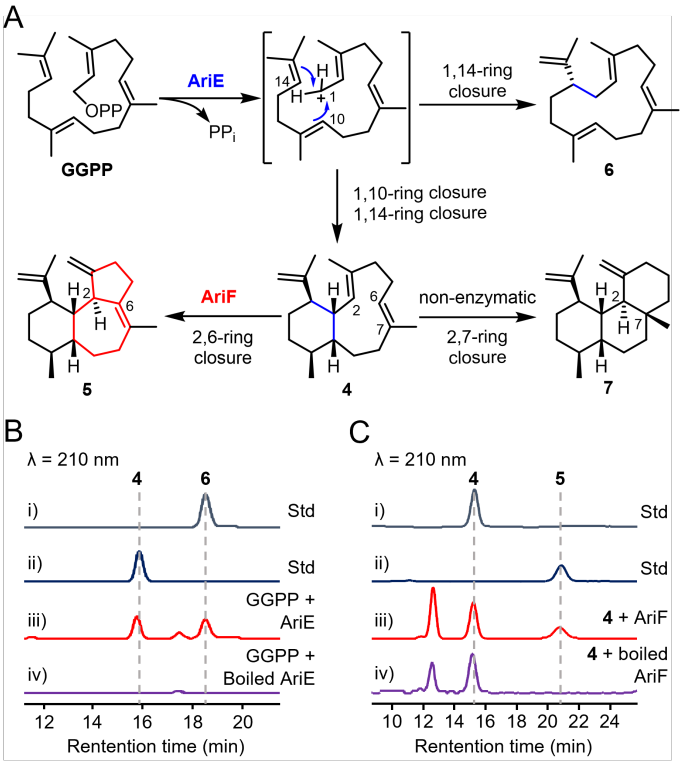

Figure 3. Biochemical characterizations of AriE and AriF. (A) Scheme of the reactions of AriE and AriF. (B) HPLC profiles of the *in vitro* reactions of AriE with GGPP. (C) HPLC profiles of the *in vitro* reactions of AriF with benditerpe-2,6,15-triene (**4**).

AriF, a P450, Mediates Cyclization of the Eunicellane Scaffold into the 6/7/5-Tricyclic Aridacins. Since **4** accumulated in the Δ*ariF* mutant, we proposed that the P450 AriF catalyzes the third ring formation immediately after terpene cyclization. To test this hypothesis, we cloned a codon-optimized version of *ariF* into *E. coli* DL10026, the producer of **4**, with the redox partner RhFRed to yield *E. coli* DL10028. Besides **4**, DL10028 produced a new compound with an identical retention time with that of **5** seen in the Δ*ariF* mutant **(Figure 2F)**. A large-scale (30-L) fermentation was performed to collect 3 mg of **5**. The GC-MS of **5** showed a molecular ion peak at *m/z* 270.17 (**Figure S57**), corresponding to a diterpene hydrocarbon of molecular formula $C_{20}H_{30}$ with six degrees of unsaturation. Its 1D and 2D NMR spectra suggested that **5** was an analogue of aridacin A (**1**) with an isopropenyl group in place of the glyceric acid side chain in **1** (**Figures S58–S63** and **Table S12**). This structural difference was supported by ^{1}H NMR data (δ_H 4.85 and 4.81, C$\underline{H_2}$16; 1.65, C$\underline{H_3}$17) and ^{13}C NMR data (δ_C 147.8, $\underline{C}$15; 110.7, $\underline{C}H_2$16; and 21.7, $\underline{C}H_3$17). Thus, **5** was assigned as a 6/7/5-fused tricyclic diterpene and named arida-3,6,15-triene.

To obtain direct evidence that AriF catalyzes the unusual cyclization of **4** into **5**, we sought to confirm enzymatic activity via *in vitro* experiments. Unfortunately, due to unsuccessful expression of either wild-type or codon-optimized *ariF* in *E. coli*, we produced AriF in *S. albus* J1074 (**Figure S64**). AriF was assayed in the presence of **4**, NADPH, and potential redox partners (CamA/CamB, RhfRed, or FdR/Fdx).[40] AriF produced a single enzymatic product **5** when paired with either CamA/CamB or RhfRed, with much higher production of **5** observed with CamA/CamB (**Figures 3C and S65**). Overall, the data conclusively supports that the nascent 6/7/5-fused tricyclic skeleton of **1–3** is created by a step-wise combination of a class I TC (AriE) and P450 (AriF), an unprecedented event in the biosynthesis of core terpene skeletons.

Quantum Chemical Calculations Support the Carbocation Cyclization Mechanism of AriF. The P450-catalyzed conversion of **4** to **5** resembles the terpene cyclization of VrtK and rearrangements of PenM/PntM and *Tw*CYP71BE86, where oxidation of a radical provides a

carbocation for cyclization.[18–21] We initially proposed two possible pathways (**Figure 4**). In pathway (i), AriF abstracts a hydrogen from CH_3-20 of **4** via Compound I to yield radical intermediate **a**, which undergoes electron transfer rather than oxygen rebound to form allylic carbocation **b**. A subsequent 2,6-ring closure yields the tricyclic skeleton with deprotonation at C-6 providing **5**. In pathway (ii), hydrogen abstraction and cation formation occur at C-4 followed by a 1,3-hydride shift to form intermediate **b**; cyclization and deprotonation then follow that in pathway (i).

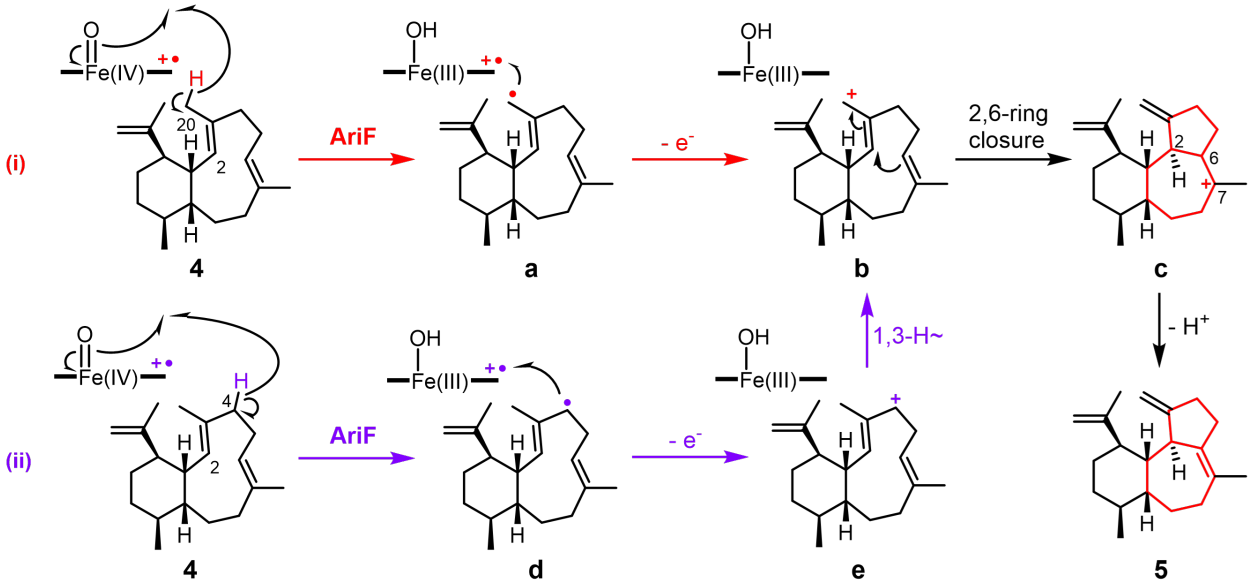

Figure 4. Putative catalytic mechanism of AriF.

Quantum chemical computations were executed to examine the possible cyclization mechanisms (**Figure 4**). Geometry optimizations and energies were obtained using the mPW1PW91/6-31+G(d,p) density functional theory method,[41–44] which has been used extensively for modeling terpene-forming carbocation reactions.[45–47] Structures for radicals **a** and **d** were readily located. A transition state structure for the 1,3-H shift that interconverts radicals a and d was also located, but the barrier for that shift is predicted to be very large (>50 kcal/mol). While a structure for carbocation **c** was readily located, attempts to locate **b** and **e** with the relative stereochemical configuration corresponding to **5** led directly to structures with 6/7/5-fused tricyclic frameworks,

i.e., **c** was formed when attempting to locate **b** and its analog when attempting to locate **e**. These results suggest that the cations formed from radicals **a** and **d** have their π-bonds and cation centers so close in space that there is no barrier for them to combine. In addition, since product **5** is observed, rather than a product of direct cyclization of carbocation **e** (i.e., 6/7/5 tricycle with an alkene between C-3 and C-4), it seems plausible that initial hydrogen abstraction occurs at C-20. Altogether, pathway (i) is supported as the most likely mechanistic route for AriF cyclization of the *cis*-eunicellane skeleton of **4** into arida-3,6,15-triene (**5**).

Conclusion

Most of the skeletal diversity of terpenes in nature are generated by TCs, enzymes that generate structurally and stereochemically complex polycyclic hydrocarbons from acyclic precursors. However, the enzymatic repertoire capable of performing terpene cyclization is far more diverse than a single enzyme family.[17] In this study, we used genome mining and discovered a new class of highly oxidized eunicellane-derived 6/7/5-fused tricyclic diterpenoids aridacins A−C (**1**−**3**) from the thermophilic actinomycete *A. arida*. Heterologous production, *in vivo* inactivation, and *in vitro* enzyme characterization systematically established that a TC and P450, AriE and AriF, respectively, successively generate the 6/10-fused bicyclic *cis*-eunicellane skeleton and the 6/7/5-fused tricyclic scaffold. Quantum chemical computations supported the proposal that AriF catalyzes a carbocation mechanism for the third ring formation. Although three P450s have been previously reported to mediate terpene rearrangements or cyclization in (mero)terpenoid biosynthesis, they all function toward the end of their biosynthetic pathways. In the biosynthesis of the aridacins, a TC and P450 work in tandem to initially create the backbone of the aridacins, an unprecedented strategy in terpene skeletal construction. Our discovery expands the catalytic capacity and diversity of P450s and sets the stage for future efforts to investigate the inherent principles of carbocation generation by P450s in the biosynthesis of terpenoids. During submission of this manuscript, *ariD–G* was heterologously expressed in *S. albus* J1074M producing a benditerpenoic acid-like eunicellane diterpenoid.[8,48] The production of our 6/7/5-tricyclic

diterpenoids and the 6/10-bicyclic product from the same set of genes raises an intriguing question of how the *ari* BGC is being controlled in different heterologous hosts and what are the genuine natural products from the original strain *A. arida*.

Acknowledgments

We wish to thank Profs. Ning-Hua Tan from China Pharmaceutical University and Hui Ming Ge from Nanjing University for generous access to the GC-MS and HRESIMS equipment, respectively. We are grateful to Profs. Shengying Li from Shandong University and Hans Renata from Rice University for kind providing plasmids pET28a(+)-Fdx and pET28a(+)-FdR, and pET28a(+)-RhfRed and pETduet-1-Opt13, respectively. D.J.T. gratefully acknowledges the NSF XSEDE program. This work is supported in part by the National Science Foundation of China Grant 82073746 (L.-B.D.), the National Institutes of Health Grants R00 GM124461 (J.D.R.) and R35 GM142574 (J.D.R.), the Thousand Youth Talents Program of China (L.-B.D.), the Jiangsu Specially Appointed Professor Program (L.-B.D.), the Jiangsu Funding Program for Excellent Postdoctoral Talent Program (Q.Y.), and the Postgraduate Research & Practice Innovation Program of Jiangsu Province (Z.W.).

Author contributions

L.-B.D. conceived the project; Z.W., Q.Y., D.J.T., and L.-B.D. designed the experiments; Z.W., Q.Y., J.H., H.L., X.P., and H.-M.X. performed the experiments; Z.W., Q.Y., Z.L., J.D.R., D.J.T., and L.-B.D. analyzed the results; Z.W., Q.Y., J.D.R., D.J.T., and L.-B.D. wrote the paper with inputs from all co-authors.

Competing financial interests

The authors declare no competing financial interest.

Correspondence and requests for materials should be addressed to Q.Y., D.J.T., or L.-B.D.

References

(1) Li, G.; Dickschat, J. S.; Guo, Y.-W. Diving into the world of marine 2,11-cyclized cembranoids: a summary of new compounds and their biological activities. *Nat. Prod. Rep.* **2020**, *37*, 1367–1383.

(2) Welford, A. J.; Collins, I. The 2,11-cyclized cembranoids: cladiellins, asbestinins, and briarellins (period 1998–2010). *J. Nat. Prod.* **2011**, *74*, 2318–2328.

(3) Burkhardt, I.; de Rond, T.; Chen, P. Y.; Moore, B. S. Ancient plant-like terpene biosynthesis in corals. *Nat. Chem. Biol.* **2022**, *18*, 664–669.

(4) Scesa, P. D.; Lin, Z.; Schmidt, E. W. Ancient defensive terpene biosynthetic gene clusters in the soft corals. *Nat. Chem. Biol.* **2022**, *18*, 659–663.

(5) Pinto, A. C.; Pizzolatti, M. G.; Epifanio, R. d. A.; Frankmölle, W.; Fenical, W. The isolation of novel diterpenoids, including a C40 *bis*-diterpenoid, from the Brazilian plant *Vellozia magdalenae* (Velloziaceae). *Tetrahedron.* **1997**, *53*, 2005–2012.

(6) Zhang, B.-Y.; Wang, H.; Luo, X.-D.; Du, Z.-Z.; Shen, J.-W.; Wu, H.-F.; Zhang, X.-F. Bisyinshanic acids A and B, Two novel diterpene dimers from the roots of *Euphorbia yinshanica*. *Helv. Chim. Acta.* **2012**, *95*, 1672–1679.

(7) Ma, L.-F.; Chen, M.-J.; Liang, D.-E.; Shi, L.-M.; Ying, Y.-M.; Shan, W.-G.; Li, G.-Q.; Zhan, Z.-J. *Streptomyces albogriseolus* SY67903 produces eunicellin diterpenoids structurally similar to terpenes of the gorgonian *muricella sibogae*, the bacterial source. *J. Nat. Prod.* **2020**, *83*, 1641–1645.

(8) Zhu, C.; Xu, B.; Adpressa, D. A.; Rudolf, J. D.; Loesgen, S. Discovery and biosynthesis of a structurally dynamic antibacterial diterpenoid. *Angew. Chem. Int. Ed. Engl.* **2021**, *60*, 14163–14170.

(9) Chen, B.-W.; Chao, C.-H.; Su, J.-H.; Tsai, C.-W.; Wang, W.-H.; Wen, Z.-H.; Huang, C.-Y.; Sung, P.-J.; Wu, Y.-C.; Sheu, J.-H. Klysimplexins I-T, eunicellin-based diterpenoids from the cultured soft coral *Klyxum simplex*. *Org. Biomol. Chem.* **2011**, *9*, 834–844.

(10) Hassan, H. M.; Khanfar, M. A.; Elnagar, A. Y.; Mohammed, R.; Shaala, L. A.; Youssef, D. T.; Hifnawy, M. S.; El Sayed, K. A. Pachycladins A-E, prostate cancer invasion and migration inhibitory Eunicellin-based diterpenoids from the red sea soft coral *Cladiella pachyclados*. *J. Nat. Prod.* **2010**, *73*, 848–853.

(11) Chen, X.-T.; Bhattacharya, S. K.; Zhou, B.; Gutteridge, C. E.; Pettus, T. R. R.; Danishefsky, S. J. The total synthesis of eleutherobin. *J. Am. Chem. Soc.* **1999**, *121*, 6563–6579.

(12) Xu, B.; Tantillo, D. J.; Rudolf, J. D. Mechanistic insights into the formation of the 6,10-bicyclic eunicellane skeleton by the bacterial diterpene synthase Bnd4. *Angew. Chem. Int. Ed. Engl.* **2021**, *60*, 23159–23163.

(13) Li, Z. N., Xu, B. F., Kojasoy, V., Ortega, Teresa., Adpressa, D. A, Ning, W. B., Wei, X. T., Liu, J. M., Tantillo, D. J., Loesgen, Sandra., Rudolf, J. D. First trans-eunicellane terpene synthase in bacteria. *Chem.* **2023**, 10.1016/j.chempr.2022.12.006.

(14) Christianson, D. W. Structural and chemical biology of terpenoid cyclases. *Chem. Rev.* **2017**, *117*, 11570–11648.

(15) Tang, M.-C.; Zou, Y.; Watanabe, K.; Walsh, C. T.; Tang, Y., Oxidative cyclization in natural product biosynthesis. *Chem. Rev.* **2017**, *117*, 5226–5333.

(16) Rudolf, J. D.; Chang, C.-Y.; Ma, M.; Shen, B. Cytochromes P450 for natural product biosynthesis in *Streptomyces*: sequence, structure, and function. *Nat. Prod. Rep.* **2017**, *34*, 1141–1172.

(17) Rudolf, J. D.; Chang, C.-Y. Terpene synthases in disguise: enzymology, structure, and opportunities of non-canonical terpene synthases. *Nat. Prod. Rep.* **2020**, *37*, 425–463.

(18) Zhu, D.; Seo, M.-J.; Ikeda, H.; Cane, D. E. Genome mining in *Streptomyces*. Discovery of an unprecedented

P450-catalyzed oxidative rearrangement that is the final step in the biosynthesis of pentalenolactone. *J. Am. Chem. Soc.* **2011**, *133*, 2128–2131.
(19) Duan, L.; Jogl, G.; Cane, D. E. The cytochrome P450-catalyzed oxidative rearrangement in the final step of pentalenolactone biosynthesis: substrate structure determines mechanism. *J. Am. Chem. Soc.* **2016**, *138*, 12678–12689.
(20) Hansen, N. L.; Kjaerulff, L.; Heck, Q. K.; Forman, V.; Staerk, D.; Møller, B. L.; Andersen-Ranberg, J. *Tripterygium wilfordii* cytochrome P450s catalyze the methyl shift and epoxidations in the biosynthesis of triptonide. *Nat. Commun.* **2022**, *13*, 5011.
(21) Chooi, Y.-H.; Hong, Y. J.; Cacho, R. A.; Tantillo, D. J.; Tang, Y. A cytochrome P450 serves as an unexpected terpene cyclase during fungal meroterpenoid biosynthesis. *J. Am. Chem. Soc.* **2013**, *135*, 16805–16808.
(22) Faylo, J. L.; Ronnebaum, T. A.; Christianson, D. W. Assembly-Line catalysis in bifunctional terpene synthases. *Acc. Chem. Res.* **2021**, *54*, 3780–3791.
(23) Rudolf, J. D.; Alsup, T. A.; Xu, B.; Li, Z. Bacterial terpenome. *Nat. Prod. Rep.* **2021**, *38*, 905–980.
(24) Wilson, Z. E.; Brimble, M. A. Molecules derived from the extremes of life: a decade later. *Nat. Prod. Rep.* **2021**, *38*, 24–82.
(25) Mao, J.; Wang, J.; Dai, H.-Q.; Zhang, Z.-D.; Tang, Q.-Y.; Ren, B.; Yang, N.; Goodfellow, M.; Zhang, L.-X.; Liu, Z.-H. *Yuhushiella deserti* gen. nov., sp. nov., a new member of the suborder *Pseudonocardineae*. *Int. J. Syst. Evol. Microbiol.* **2011**, *61*, 621–630.
(26) Nouioui, I.; Carro, L.; García-López, M.; Meier-Kolthoff, J. P.; Woyke, T.; Kyrpides, N. C.; Pukall, R.; Klenk, H.-P.; Goodfellow, M.; Göker, M. Genome-Based taxonomic classification of the phylum *Actinobacteria*. *Front. Microbiol.* **2018**, *9*, 2007.
(27) Dong, L.-B.; Zhang, X.; Rudolf, J. D.; Deng, M.-R.; Kalkreuter, E.; Cepeda, A. J.; Renata, H.; Shen, B. Cryptic and stereospecific hydroxylation, oxidation, and reduction in platensimycin and platencin biosynthesis. *J. Am. Chem. Soc.* **2019**, *141*, 4043–4050.
(28) Dong, L.-B.; Rudolf, J. D.; Deng, M.-R.; Yan, X.; Shen, B. Discovery of the tiancilactone antibiotics by genome mining of atypical bacterial type II diterpene synthases. *ChemBioChem.* **2018**, *19*, 1727–1733.
(29) Yabuuchi, T.; Kusumi, T. Phenylglycine methyl ester, a useful tool for absolute configuration determination of various chiral carboxylic acids. *J. Org. Chem.* **2000**, *65*, 397–404.
(30) Deposition Number 2216506 (for **1a**) contains the supplementary crystallographic data for this paper. This data is provided free of charge by the joint Cambridge Crystallographic Data Centre and FIZ Karlsruhe Access Structures service.
(31) Yamada, Y.; Arima, S.; Nagamitsu, T.; Johmoto, K.; Uekusa, H.; Eguchi, T.; Shin-ya, K.; Cane, D. E.; Ikeda, H. Novel terpenes generated by heterologous expression of bacterial terpene synthase genes in an engineered *Streptomyces* host. *J. Antibiot.* **2015**, *68*, 385–394.
(32) Yamada, Y.; Kuzuyama, T.; Komatsu, M.; Shin-Ya, K.; Omura, S.; Cane, D. E.; Ikeda, H. Terpene synthases are widely distributed in bacteria. *Proc. Natl. Acad. Sci. U.S.A.* **2015**, *112*, 857–862.
(33) Li, G.; Guo, Y. W.; Dickschat, J. S. Diterpene biosynthesis in *Catenulispora acidiphila*: On the mechanism of catenul-14-en-6-ol synthase. *Angew. Chem. Int. Ed. Engl.* **2021**, *60*, 1488–1492.
(34) Vyry Wouatsa, N. A.; Misra, L. N.; Venkatesh Kumar, R.; Darokar, M. P. Tchoumbougnang, F. Zantholic acid, a new monoterpenoid from *Zanthoxylum zanthoxyloides*. *Nat. Prod. Res.* **2013**, *27*, 1994–1998.
(35) Li, F.-R.; Lin, X.; Yang, Q.; Tan, N.-H.; Dong, L.-B. Efficient production of clerodane and *ent*-kaurane diterpenes through truncated artificial pathways in *Escherichia coli*. *Beilstein. J. Org. Chem.* **2022**, *18*, 881–888.

(36) Pan, X.; Du, W.; Zhang, X.; Lin, X.; Li, F.-R.; Yang, Q.; Wang, H.; Rudolf, J. D.; Zhang, B.; Dong, L.-B. Discovery, structure, and mechanism of a class II sesquiterpene cyclase. *J. Am. Chem. Soc.* **2022**. *144*, 22067–22074.
(37) Schwabe, R.; Farkas, I.; Pfander, H. Synthesis of (−)-(*R*)-nephthenol and (−)-(*R*)-cembren A. *Helv. Chim. Acta.* **1988**, *71*, 292–297.
(38) Rinkel, J.; Lauterbach, L.; Rabe, P.; Dickschat, J. S. Two diterpene synthases for spiroalbatene and cembrene A from *Allokutzneria albata*. *Angew. Chem. Int. Ed. Engl.* **2018**, *57*, 3238–3241.
(39) Angulo-Preckler, C.; Genta-Jouve, G.; Mahajan, N.; de la Cruz, M.; de Pedro, N.; Reyes, F.; Iken, K.; Avila, C.; Thomas, O. P. Gersemiols A–C and eunicellol A, diterpenoids from the arctic soft coral *gersemia fruticosa*. *J. Nat. Prod.* **2016**, *79*, 1132–1136.
(40) Li, S.; Du, L.; Bernhardt, R. Redox partners: Function modulators of bacterial P450 enzymes. *Trends. Microbiol.* **2020,** *28*, 445–454.
(41) Lee, C.; Yang, W.; Parr, R. G. Development of the Colle-Salvetti correlation-energy formula into a functional of the electron density. *Phys. Rev. B.* **1988**, *37*, 785–789.
(42) Adamo, C.; Barone, V. Exchange functionals with improved long-range behavior and adiabatic connection methods without adjustable parameters: The m PW and m PW1PW models. *J. Chem. Phys.* **1998**, *108*, 664–675.
(43) Matsuda, S. P.; Wilson, W. K.; Xiong, Q. Mechanistic insights into triterpene synthesis from quantum mechanical calculations. Detection of systematic errors in B3LYP cyclization energies. *Org. Biomol. Chem.* **2006**, *4*, 530–543.
(44) Frisch, M.; Trucks, G.; Schlegel, H.; Scuseria, G.; Robb, M.; Cheeseman, J.; Scalmani, G.; Barone, V.; Petersson, G.; Nakatsuji, H. et al. Gaussian 16; Gaussian Inc., Wallingford, CT, 2016.
(45) Tantillo, D. J. Biosynthesis via carbocations: Theoretical studies on terpene formation. *Nat. Prod. Rep.* **2011**, *28*, 1035–1053.
(46) Tantillo, D. J. Exploring terpenoid biosynthesis with quantum chemical computations. *Compr. Nat. Prod. III***2020**, 1, 644–653.
(47) A data set collection of computational results (DOI: 10.19061/iochem-bd-6-224) is available at the IoChem-BD repository (Álvarez-Moreno, M.; de Graaf, C.; López, N.; Maseras, F.; Poblet, J. M.; Bo, C. Managing the computational chemistry big data problem: The ioChem-BD platform. *J. Chem. Inf. Model.* **2015**, 55, 95–103) and can be accessed via https://iochem-bd.bsc.es/browse/handle/100/280454.
(48) Hu, Y. L.; Zhang, Q.; Liu, S. H.; Sun, J. L.; Yin, F. Z.; Wang, Z. R.; Shi, J.; Jiao, R. H.; Ge, H. M. Building *Streptomyces albus* as a chassis for synthesis of bacterial terpenoids. *Chem. Sci.* **2023**, 10.1039/D2SC06033G.